MATHEMATICAL BIOSCIENCES
AND ENGINEERING
Volume **10**, Number **4**, August **2013**

doi:10.3934/mbe.2013.10.1227

pp. **1227–1251**

MITIGATION OF EPIDEMICS IN CONTACT NETWORKS THROUGH OPTIMAL CONTACT ADAPTATION

Mina Youssef

K-State Epicenter, Department of Electrical and Computer Engineering
Kansas State University
2061 Rathbone Hall, Manhattan, KS 66506-5204, USA
and
Network Dynamics and Simulation Science Laboratory
Virginia Bioinformatics Institute, Virginia Tech
Research Building XV, 1880 Pratt Drive, Blacksburg, VA 24061, USA

Caterina Scoglio

K-State Epicenter, Department of Electrical and Computer Engineering
Kansas State University
2061 Rathbone Hall, Manhattan, KS 66506-5204, USA

(Communicated by Haiyan Wang)

Abstract. This paper presents an optimal control problem formulation to minimize the total number of infection cases during the spread of susceptible-infected-recovered SIR epidemics in contact networks. In the new approach, contact weighted are reduced among nodes and a global minimum contact level is preserved in the network. In addition, the infection cost and the cost associated with the contact reduction are linearly combined in a single objective function. Hence, the optimal control formulation addresses the trade-off between minimization of total infection cases and minimization of contact weights reduction. Using Pontryagin theorem, the obtained solution is a unique candidate representing the dynamical weighted contact network. To find the near-optimal solution in a decentralized way, we propose two heuristics based on Bang-Bang control function and on a piecewise nonlinear control function, respectively. We perform extensive simulations to evaluate the two heuristics on different networks. Our results show that the piecewise nonlinear control function outperforms the well-known Bang-Bang control function in minimizing both the total number of infection cases and the reduction of contact weights. Finally, our results show awareness of the infection level at which the mitigation strategies are effectively applied to the contact weights.

1. **Introduction.** In the last decade, epidemic modeling has allowed heterogeneity into models due to increasing computational capabilities. Correspondingly, complex networks are amongst the primary mathematical tools used to express heterogeneity in epidemic models [31, 30], representing either the contact networks among individuals or the movement networks among sub-populations. Moreover, epidemic models have been developed at multiple spatial and temporal scales from the very detailed agent-based simulations [4] to the global meta-population computational

2010 *Mathematics Subject Classification.* Primary: 58F15, 58F17; Secondary: 53C35.

Key words and phrases. Spread of epidemics, optimal control of epidemics, adaptive contact networks, network-based approach, behavioral responses.

tools [9, 1]. Recent models take into account accurately the structure and the statistical characteristics of the population, both in urban [13] and rural [38] areas. However, one of the most important applications of epidemic modeling is the testing and evaluation of mitigation strategies and their costs [40]. For example, consider the classical problem in epidemiology of optimal vaccination distribution given limited resources. Such a problem is resolved through epidemic modeling and numerical simulations. In this context, however, the still common assumption that the contact network is static is very primitive, and it can produce inaccurate modeling results. As a matter of fact, during an epidemic, contact patterns are modified, and these modifications in turn modify the epidemic evolution [11]. The two intertwined dynamic processes, the one related to the epidemic spreading and the other related to the contact network adaptation, act together and impact the epidemic size. Thus, mitigation strategies, which include social distancing, a reduction in the normal contact of individuals, cannot be represented correctly without taking into account a time varying contact network. Moreover, in social distancing intervention, some contacts are eliminated from the network to reduce the spread of infection. However, what if the contacts have a lower bound that is greater than 0? In other words, individuals are not fully isolated during the wave of an epidemic and sometimes do not comply with the announced interventions. Thus, how can we model a weight reduction intervention that does not isolate individuals from the network? If there is a cost accompanied with weight reduction, how to balance the weight reduction cost and the infection cost?

In this paper, we answer these questions by engaging the optimal control theory with the well-known susceptible-infected-recovered SIR compartmental model. We assume a hypothetical SIR epidemic that spreads in a contact network composed of nodes and links. Nodes represent individuals, while links represent contacts among the individuals. We formulate a continuous time optimal control problem in which total infection size is minimized due to the dynamic change in the contact weights among nodes. To apply the optimal control theory, we consider the spread of an SIR epidemic in the network as a dynamical system, and the total number of infected cases as the state of the system, while the control function is the weight reduction of the contact network leading to slow/reduce spread of the epidemic. Therefore, the control function is the weight reduction, while the state variables are the states of each node, namely susceptible, infected and recovered. Hence, the main objective is to minimize both total infection size in the contact network and weight reduction. Pontryagin theorem [32] is used to provide necessary conditions of optimality. Thus, the obtained solution represents a unique candidate (extremal) to give the optimal solution. Consequently, the candidate solution represents a dynamical weighted network. To obtain near optimal decentralized solutions, which can represent spontaneous behavioral responses, we propose two heuristics in which two distinct control functions are defined based on the Bang-Bang controller and a nonlinear piecewise controller, respectively. The optimal control formulation and the heuristics are numerically evaluated on different contact network structures, showing the effectiveness and implementability of the proposed methods.

We summarize our contribution in the following ways:

- Proposing an optimal control approach for mitigation strategies to SIR epidemics in contact networks
- Considering realistic scenarios in contact networks
- Proposing two heuristics to find near optimal solutions

The paper is organized as follows: In Section 2, we review the literature and in Section 3, we present the network-based SIR approach. The optimal control problem is discussed in detail in Section 4, while in Section 5 we propose computational heuristics to find decentralized solutions. Extensive numerical evaluations for the computational heuristics using preferential attachment networks and a survey-based contact network are presented in Section 6, followed by a discussion and a summary in Sections 7 and 8, respectively. Finally we conclude and discuss future work in Section 9.

2. **Literature review.**

The work in [24] addressed the effect of quarantine strategy on the spread of SIR epidemics. The quarantine strategy assumes that the susceptible nodes disconnect their contacts with the infected neighbors and reconnect with other susceptible neighbors with a given probability. Using the rewiring approach, the authors found a phase transition at a critical rewiring probability below which a large number of nodes are infected. Our approach is different from that of [24] since nodes do not terminate their daily contacts with the infected neighbors, and they create new contacts with new nodes; however, susceptible nodes do reduce their contact frequency with infected neighbors.

Gao and Ruan in [16] studied the effect of human movement on the spread of infectious SIS epidemics, confirming the existence of reproductive number below which a disease does not spread out.

Gross and Blasius highlighted the research in adaptive networks as shown in [18] with two major lines. The first line is related to the dynamics of networks such that a topology evolves over time revealing many indigenous characteristics. The second line is that in the dynamics on networks, the states of the nodes in the network change with time. Additionally, the relationship between the dynamics of networks and the dynamics on networks was studied showing a feedback loop between the state of the nodes and the topology. In addition, Gross et al.in [19] discussed the spread of epidemics on networks, and how the network can become adaptive by rewiring the links according to the state of the nodes. The authors concluded that the local effect of rewiring suppresses the epidemic, while the topological effect increases the chance of the epidemic spreading.

Jiang and Dong in [21] proposed an optimal concept of control measures to control the spread of SARS outbreaks in minimum time. They found that the optimal control is the Bang-Bang function when the objective is to minimize the lifetime of an outbreak. However, they only focused on a subsystem of the compartmental model, which only includes the exposed class and the infectious class.

V. Marceau *et al.* studied the coevolution of SIS disease and network topology simultaneously in [26], introducing an adaptive rewiring rule through which the topology changes with time. They found that during the initial phase of an epidemic, the number of links that connect susceptible nodes with infectious nodes drops quickly, and hence the susceptible nodes compose a strong community connected with very few infectious nodes. Eventually, the epidemic invades the well connected susceptible community causing a sharp drop in the number of links in the susceptible community.

Prakash *et al.* studied virus propagation in time-varying networks in [33]. They divided the time unit into two periods with each period having its own network adjacency matrix representing the binary contacts among the nodes. They found that the epidemic threshold is the reciprocal of the maximum eigenvalue of the

multiplication of the two system matrices representing the two periods. They also extended the same concept to general alternative behaviors during the lifetime of the virus. In addition, the authors proposed various mitigation strategies based on topological characteristics of the networks. Bondes *et al.* [7] studied the relationship between communicable diseases and the evolution of social systems. They proposed a game theory approach to find the social behavior of a host during the life cycle of communicable diseases. In addition, the authors presented the relationship between the strength of the diseases and the contact rates of the hosts.

Reluga addressed the effect of social distancing on the spread of SIR epidemics [36, 35]. For example, he used differential game theory to find the social distancing pattern in population-based model [36, 35]. The solution represents the equilibrium at which excess social distancing does not improve the solution.

The authors in [37] addressed the optimal control of SIS epidemics in two coupled subpopulations and determined the optimal mitigation strategy when scarce resources are available based on the Hamiltonian method. The authors also found that the optimal solution represents the distribution of scarce resources in large susceptible subpopulation with the least infection cases to reduce the force of infection.

The work in [8] addressed the optimal vaccination strategy against the human papillomavirus (HPV). The optimal strategy is to find the best target for vaccination. The authors found that the solution obtained using optimal control theory is more efficient than the solution obtained from constant control strategy; this is because the optimal solution leads to control the disease at steady state.

Volz and Meyers [41] addressed dynamic contacts among nodes during the outbreak of SIR epidemics, proposing a dynamic contact pattern such that every node preserves a constant number of neighbors at any time. Each contact is temporary, and it lasts a variable time duration, after which that contact is replaced by a new neighbor.

Optimal control theory was used to evaluate the best policies to control the spread of seasonal and novel A-H1N1 strains [34]. The controller is a function of social distancing cost and the antiviral treatment policies cost. The authors concluded that social distancing policies can reduce the infection size by more than 99%, which is theoretically possible when the population is isolated with scarce resources althought it is unrealistic.

Fenichel *et al.* [14] studied adaptive human behavior during the spread of SIR epidemics. In their models, contacts are classified based on population states, i.e. contacts between susceptible and infected states, contact between susceptible and recovered states and so on. The authors proposed a dynamic programming problem, which addresses the tradeoff between the contact benefits and the infection cost. An emperical study on the spread of epidemics in dynamical contact networks were addressed in [39]. The authors collected data about the face-to-face contacts and duration per contact between pair of individuals that are within a certain distance. By establishing a contact network that changes with time, the authors studied the spread of SEIR epidemics and they showed the importance of including the heterogeneity of the contact duration. The authors in [12] studied the spread of flu in small population by collecting data about the individuals' daily symptoms. The authors were able to fit the collected symptom data to SIS like -disease. Such study gives insights about the relationship between the proximity of individuals and the spread of flu. The authors in [20] studied the impact of the experiment design in collecting contact data and the duration of the study on the outcome of

an epidemic spreading process. The authors illustrated the correlation between the dynamcis of empirical contact networks, the number of participants and the outcome of simulation models. The authors in [25] addressed a practical intervention for household contacts. The authors proposed that every infected individual will only has a single contact with the care giver. The authors found that the overall infected cases are reduced by a constant value for different transmissibility values. The authors in [23] studied the contact tracing to isolate nodes with infectious contacts. Through stochastic simulations, they investigated the effect of correlated networks on the spread of epidemics and contact contact tracing efficacy. They found that contact tracing has a better performance for assortative mixing with large epidemic size and low tracing rate, while for disassortative networks, contact tracing performs better at higher contact rates.

3. **Network-based SIR approach.** In the network-based approach, given a network with N nodes and L links, each node can be either susceptible S, infected I, or recovered R, with a given probability for each state. An infected node infects a susceptible neighbor with infection rate β, and meanwhile the infected node becomes cured with cure rate δ. The new approach is inspired by the continuous-time Markov chain SIR model, and it aims to decrease the complexity of the problem from exponential $O(3^N)$ to polynomial $O(N)$. Therefore, instead of considering the combinatorial states of the nodes in the network, we study each node specifically [42, 29] by decomposing the infinitesimal $Q_{3^N \times 3^N}$ matrix to N infinitesimal matrices $q_m(t)$ forall $m \in N$, each with three states as follows:

$$q_m(t) = \begin{bmatrix} -\beta \sum_n a_{m,n} 1_{[i_n(t)=1]} & \beta \sum_n a_{m,n} 1_{[i_n(t)=1]} & 0 \\ 0 & -\delta & \delta \\ 0 & 0 & 0 \end{bmatrix} \quad m = 1, 2, \dots N$$

where $a_{m,n}$ is the binary entry in the network adjacency matrix, representing the existence of contact between node m and node n, and the indicator function $1_{[i_m(t)=1]} = 1$ represents the event that node m is infected and 0 otherwise. In this approach, we replace the actual event of a node to be susceptible $s_m(t) = 1$ with its effective probability $S_m(t) = p(s_m(t) = 1)$, the event of a node to be infected $i_m(t) = 1$ with its effective probability $I_m(t) = p(i_m(t) = 1)$, and the event of a node to be recovered $r_m(t) = 1$ with its effective probability $R_m(t) = p(r_m(t) = 1)$. Replacing every event with its effective probability is basically a mean field approximation where $E[i_m(t)] = p(i_m(t) = 1) = I_m(t)$. Hence, the effective $\bar{q}_m(t)$ infinitesimal matrix is obtained and has the following expression:

$$\bar{q}_m(t) = \begin{bmatrix} -\beta \sum_n a_{m,n} I_n(t) & \beta \sum_n a_{m,n} I_n(t) & 0 \\ 0 & -\delta & \delta \\ 0 & 0 & 0 \end{bmatrix} \quad m = 1, 2, \dots N.$$

For every node m, we derive a system of differential equations using the effective $\bar{q}_m(t)$ infinitesimal matrix as follows:

$$\frac{d\mathcal{S}_m^T(t)}{dt} = \mathcal{S}_m^T(t) \bar{q}_m(t) \tag{1}$$

where $\mathcal{S}_m^T(t) = [S_m(t)\ I_m(t)\ R_m(t)]$ is the vector of the state probabilities of node m. The obtained differential equations are as follows:

$$\frac{dS_m(t)}{dt} = -S_m(t)\beta \sum_{n=1}^{N} a_{m,n} I_n(t), \tag{2}$$

$$\frac{dI_m(t)}{dt} = S_m(t)\beta \sum_{n=1}^{N} a_{m,n} I_n(t) - \delta I_m(t), \tag{3}$$

$$\frac{dR_m(t)}{dt} = \delta I_m(t) \quad m = 1, 2, \ldots N. \tag{4}$$

At any time t, each node m is in any of the states with a total probability of 1 so that $S_m(t) + I_m(t) + R_m(t) = 1$. In addition, the sum of rates of changes in the state probabilities equals 0 so that $\frac{dS_m(t)}{dt} + \frac{dI_m(t)}{dt} + \frac{dR_m(t)}{dt} = 0$. Therefore, we only need to solve $2N$ simultaneous differential equations instead of $3N$.

3.1. **Weighted network-based model.** Traditionally, any contact network is a weighted graph representing the contact frequency and the proximity among the nodes. We denote the contact weight between nodes m and n at time t $w_{m,n}(t)$ such that $0 \leq w_{m,n}(t) \leq 1$. The spread of infectious disease takes place in contact networks due to the contacts among susceptible and infected nodes. Therefore, the actual infection rate from an infected node n towards a susceptible node m at time t becomes $\beta w_{m,n}(t)$. Using the system of differential equations (2-4), we obtain the following SIR epidemic approach for a weighted network:

$$\frac{dS_m(t)}{dt} = -S_m(t)\beta \sum_{n=1}^{N} w_{m,n}(t) I_n(t), \tag{5}$$

$$\frac{dI_m(t)}{dt} = S_m(t)\beta \sum_{n=1}^{N} w_{m,n}(t) I_n(t) - \delta I_m(t), \tag{6}$$

$$\frac{dR_m(t)}{dt} = \delta I_m(t) \quad m = 1, 2, \ldots N. \tag{7}$$

Differential equations in (5 - 7) represent the system of equations in the optimal control formulation to minimize both the total number of infected cases and the reduction in contact weights.

4. **Optimal dynamical weights.** In this section, we formulate a continuous time optimal control problem to minimize the total infection size by properly reducing the contact weights among nodes within a finite time interval $t \in [0, T_f]$. Meanwhile, our objective is to minimize the weight reduction with respect to original epidemic-free contact weights ($t = 0$). Initially, we assume that there is no weight reduction in the contact network at time $t = 0$; however, for $t > 0$, the contact network can become a directed weighted graph in which $w_{m,n}(t)$ can be different from $w_{n,m}(t)$. During the spread of an epidemic, $t > 0$, weights are reduced from their initial epidemic-free values $w_{n,m}(0)$. In particular, we impose two bounds on each weight (m, n): a) $\alpha w_{m,n}(0) \leq w_{m,n}(t)$ and b) $w_{m,n}(t) \leq w_{m,n}(0)$, where $\alpha \in [0, 1]$ is a minimum social level coefficient. These constraints have direct implications for the network as follows: First, to preserve a minimum contact level among nodes even during epidemics, and differently from the control constraint presented in [6] where the lower bound equals 0, we introduce a positive lower bound for the

TABLE 1. Definitions of the data inputs and the variables

Data input	Definition
T_f	Final time
β	Infection rate
δ	Cure rate
α	Global minimum social contact coefficient
$w_{m,n}(0)$	Initial weight $\forall\ m, n \in N$
$S_m(0)$	Initial susceptible probability of node m
$I_m(0)$	Initial infection probability of node m
Variables	**Definition**
$w_{m,n}(t)$	Link weight at time t
$S_m(t)$	The susceptible probability of node m at time t
$I_m(t)$	The infection probability of node m at time t

weights, $\alpha w_{m,n}(0) \leq w_{m,n}(t)$ where $0 < \alpha < 1$. Second, during an epidemic, the level of contact between two nodes can not increase beyond the original level $(w_{m,n}(0))$. The value of α can be selected based on the type of applications. For instance, if the contact network represents an aggregation of subpopulations, the selection of α will be crucial because it controls the lower bound of the contact frequency (travelling by airplane or commuting by ground transportation) between two subpopulation. In this case, α can have heterogeneous values depending on the subpopulations that are in contacts, and it becomes $\alpha_{m,n}$. Also, the value of α can be set to 0 when a quarrantine scenario is proposed by decision makers like closing schools and entertainment places. In such scenario, the contact within households will be strengthened among the family members. Thus, another parameter can be employed to consider the increase of contact strength within households. For simplicity, we assume that α has a global value, and we only focus on the contact weights reduction among individuals.

4.1. **Optimal control formulation.** For every node m, the infection probability $I_m(t)$ as well as the susceptible probability $S_m(t)$ are the state variables, while the weight reduction $(w_{m,n}(0) - w_{m,n}(t))$ is the control function. The data inputs and the variables are summarized in Table 1. The objective function is given by the sum of a suitable cost function of the weight reduction, and the total infection size as shown in the following equation:

$$\text{Minimize} \int_0^{T_f} \Big(\sum_{m,n \in N} [f(w_{m,n}(0) - w_{m,n}(t))] + \sum_{m \in N} \beta S_m(t) \sum_n I_n(t) w_{m,n}(t) \Big) dt \tag{8}$$

The first term $f(.)$ is a non-negative strictly convex function representing the weight reduction cost, while the second term represents new infection cases at time t. Moreover, the problem constraints are the differential equations (5) and (6) in addition to the following weight constraint:

$$\alpha w_{m,n}(0) \leq w_{m,n}(t) \leq w_{m,n}(0)\ \forall\ m, n\ \in N \tag{9}$$

The optimal control theory can be applied to any contact network having heterogeneous connectivity; however expensive numercial computation is required to obtain the candidate (extremal) solutions of the control and the state functions. Therefore, to highlight the dynamical properties of the optimal control function, we analyze the candidate solution for homogeneously-mixing networks in which every individual is in contact with all individuals in the network. The homogeneous connectivity assumption simplifies the analysis of the optimal control problem as shown below:

4.2. **Case study: Homogeneously mixing population.** Homogeneously mixing population is used to model the spread of infectious diseases in large population [2]. In addition, it is proposed to study within-household contact patterns [25, 5, 17] such that every individual has the same number of contacts with other individuals within the household. Also the homogeneous mixing approach is a very strong assumption having limited validity given the small-world nature of most human contact networks. Such networks hold heterogeneous contact patterns. In addition, the return on investment in the homogeneous mixing approach is low because the return investment is equal for every individual. In the heterogeneous contact networks, the return of investment will depend on number of contacts per individual. Further studies on the effect of heterogeneous contacts will be addressed in the future work. Due to the homogeneous assumption, the spatial index m is dropped from the susceptible probability, infection probability and the contact weight, and these variables become $S(t)$, $I(t)$, and $w(t)$, respectively. We denote the normal contact weight w_o instead of $w_{m,n}(0)$. It is worth noting that the optimization problem is nonlinear and therefore it is not convex. The objective function becomes as follows: Minimize the functional

$$J(S(t), I(t), w(t)) = \int_0^{T_f} \Big(f(w_o - w(t)) + \beta S(t) I(t) w(t) \Big) dt \tag{10}$$

The function $f(w_o - w(t))$ represents the weight reduction cost $f(0) = 0$. In addition, we assume that $f(w_o - w(t))$ is a strictly convex function. The second term represents the fraction of new infection at time t. Therefore, the main objective is to minimize a linear combination of the cost associated with the weight reduction and the infection cost for all $0 < t \leq T_f$.For homogeneously mixing population, the constraints become as follows:

$$\frac{dS(t)}{dt} = -\beta S(t) I(t) w(t), \tag{11}$$

$$\frac{dI(t)}{dt} = \beta S(t) I(t) w(t) - \delta I(t), \tag{12}$$

$$\alpha w_o \leq w(t) \leq w_o. \tag{13}$$

Hamiltonian methods and Pontryagin's minimum principle [32] are applied to different optimization problems for compartmental models [37, 8, 41, 14, 27, 28, 15] to determine the explicit optimal control function and the optimal state variables. Pontryagin theorem provides necessary conditions of optimality. Therefore, the obtained solution is the unique candidate (extremal) to give the optimal solution. We apply Pontryagin's minimum principle and we derive the Hamiltonian function

H as follows:

$$\begin{aligned} H(S(t), I(t), w(t), \lambda_I(t), \lambda_S(t)) = f(w_o - w(t)) \\ +\beta S(t)I(t)w(t) - \delta\lambda_I(t)I(t) \\ +(\lambda_I(t) - \lambda_S(t))\beta S(t)I(t)w(t). \end{aligned} \tag{14}$$

The co-state equations and the transversality conditions are as follows:

$$\frac{d\lambda_S(t)}{dt} = -\frac{\partial H}{\partial S(t)} = -\beta I(t)w(t) - (\lambda_I - \lambda_S)\beta I(t)w(t), \tag{15}$$

$$\frac{d\lambda_I(t)}{dt} = -\frac{\partial H}{\partial I(t)} = -\beta S(t)w(t) - (\lambda_I - \lambda_S)\beta S(t)w(t) + \lambda_I(t)\delta. \tag{16}$$

$$\lambda_I(T_f) = 0 \tag{17}$$

$$\lambda_S(T_f) = 0 \tag{18}$$

Next, we proceed with the optimality condition as follows:

$$H(w^*(t), S^*(t), I^*(t), \lambda_S^*(t), \lambda_I^*(t)) \leq H(w(t), S^*(t), I^*(t), \lambda_S^*(t), \lambda_I^*(t)) \tag{19}$$

where $w^*(t)$ is the candidate weight value at time t such that $H(.)$ is minimized. After substituting the Hamiltonian Eq. (14) in the optimality condition, we obtain the following inequality:

$$f(w_o - w^*(t)) + \psi^*(t)w^*(t) \leq f(w_o - w(t)) + \psi^*(t)w(t)\ \forall w(t) \in [\alpha w_o, w_o]$$

where $\psi(t) = \beta S(t)I(t)(1 + \lambda_I(t) - \lambda_S(t))$. Let $y(t) = w_o - w(t)$ represents the weight reduction such that $0 \leq y(t) \leq w_o(1-\alpha)$ and $\frac{d^2 f(y)}{dy^2} > 0$. The inequality becomes as follows:

$$f(y^*(t)) - \psi^*(t)y^*(t) \leq f(y(t)) - \psi^*(t)y(t)\ \forall y(t) \in [0, w_o(1-\alpha)] \tag{20}$$

Since $y(t) = 0$ is an admissible point and $f(y(t) = 0) = 0$, therefore, the following inequality holds for all time t:

$$f(y^*(t)) - \psi^*(t)y^*(t) \leq 0. \tag{21}$$

Since $f(y(t)) \geq 0$ and $0 \leq y(t) \leq w_o(1-\alpha)$, then:

$$f(y^*(t)) \leq \psi^*(t)y^*(t) \tag{22}$$

showing that $\psi^*(t)$ is a nonnegative function

$$\psi^*(t) = \beta S^*(t)I^*(t)(1 + \lambda_I^*(t) - \lambda_S^*(t)) \geq 0. \tag{23}$$

Since $S^*(t)$ and $I^*(t) > 0$, then:

$$1 + \lambda_I^*(t) - \lambda_S^*(t) \geq 0. \tag{24}$$

Following the analysis in [22], we propose two lemmas that are used to show the dynamic behavior of the weights in networks.

Lemma 4.1. *The co-state variable $\lambda_I^*(t)$ is nonnegative, $\lambda_I^*(t) \geq 0$ for $0 \leq t < T_f$.*

Proof. First, we apply the following function property: *for any continuous and differentiable function $g(t)$ and $g(t_1) = x$ such that for any $t > t_1$ we have $g(t) > x$, then* $\lim_{t \to t_1^+} g^{'}(t) \geq 0$. Secondly, recall that $\lambda_I^*(T_f) = \lambda_S^*(T_f) = 0$ and $\lambda_I^{*'}(T_f) = -\beta S^*(T_f)w^*(T_f)$, and $\lambda_I^{*'}(T_f) < 0$. Thirdly, we derive the proof by contradiction:

Let t_a be the time before T_f at which $\lambda_I^*(t_a) < 0$, and $\lambda_I^*(t) \geq 0$ for $t_a < t < T_f$ as follows:

$$\lim_{t \to t_a^+} \lambda_I^{*'}(t) = \lim_{t \to t_a^+} -\beta S^* w^* (1 + \lambda_I^* - \lambda_S^*) + \lambda_I^* \delta \tag{25}$$

Recall that $1 + \lambda_I^* - \lambda_S^* \geq 0$. Consequently, $\lim_{t \to t_a^+} \lambda_I^{*'}(t)$ is strictly negative, which in turns contradicts the above property. Hence, t_a does not exist. Therefore $\lambda_I^*(t) \geq 0$ for $0 < t < T_f$. □

Lemma 4.2. *The function $\psi^*(t)$ is a nonnegative concave function in time.*

Proof. The first derivative of ψ^* is as follows:

$$\begin{aligned} \psi^{*'} = \quad & (\lambda_I^{*'} - \lambda_S^{*'})\beta S^* I^* + (1 + \lambda_I^* - \lambda_S^*)\beta S^{*'} I \\ & + (1 + \lambda_I^* - \lambda_S^*)\beta S^* I^{*'} \end{aligned} \tag{26}$$

After rearrangement, it becomes as follows:

$$\psi^{*'} = -(1 - \lambda_S^*)\beta\delta S^* I^*. \tag{27}$$

Equation (15) can be rewritten as $\lambda_S^{*'}(t) = -(1 + \lambda_I^* - \lambda_S^*)\beta I^*(t) w^*(t)$. Since $1 + \lambda_I^* - \lambda_S^* \geq 0$, $\lambda_S^*(T_f) = 0$ and $\lambda_S^{*'}(T_f) < 0$, the co-state variable $\lambda_S^*(t)$ is a nonnegative decreasing function for time $0 < t < T_f$. In addition, $\lambda_S^*(t)$ function may equal 1 since $1 + \lambda_I^* - \lambda_S^* \geq 0$ and $\lambda_I^* \geq 0$. Therefore, the function $-(1 - \lambda_S^*)$ is a decreasing function in time with positive values ($\lambda_S^* > 1$), then 0 ($\lambda_S^* = 1$), then negative values ($\lambda_S^* < 1$). Also, the term $\beta\delta S^* I^*$ is positive, therefore, we concluded that $\psi^{*'}$ is a decreasing function in time from positive to negative values. Consequently, $\psi^*(t)$ is a nonnegative concave function with an inflection point in time at $\lambda_S^* = 1$. □

Based on inequality (21), and the fact that $\psi^*(t)$ is a concave function in time, we state the following theorem, which shows the candidate dynamic weight reduction in homogeneously mixing population.

Theorem 4.3. *The candidate solution of the dynamic weight reduction $y^*(t)$ during the spread of an SIR epidemic in homogeneously mixing population is as follows:*

$$y^*(t) = \begin{cases} 0 & \text{if} \quad \frac{\partial f}{\partial y}|_{y(t)=0} > \psi^*(t), \\ (\frac{\partial f}{\partial y})^{-1}(\psi^*(t)) & \text{if} \quad \frac{\partial f}{\partial y}|_{y(t)=0} \leq \psi^*(t) \leq \frac{\partial f}{\partial y}|_{y(t)=(1-\alpha)w_o}, \\ (1-\alpha)w_o & \text{if} \quad \frac{\partial f}{\partial y}|_{y(t)=(1-\alpha)w_o} < \psi^*(t). \end{cases} \tag{28}$$

Proof. From Eq. (21), $\frac{\partial(f(y(t)) - \psi(t)y(t))}{\partial y(t)}|_{y(t)=y^*(t)} = 0$ is evaluated to find the candidate weight reduction $y^*(t)$. Therefore, we obtain $y^*(t)$ as follows:

$$y^*(t) = (\frac{\partial f}{\partial y})^{-1}(\psi^*(t)) \tag{29}$$

Since inequality (21) has to be preserved for all time t, Eq. (29) is applied if and only if $\frac{\partial f}{\partial y}|_{y(t)=0} \leq \psi(t) \leq \frac{\partial f}{\partial y}|_{y(t)=(1-\alpha)w_o}$ is true. In addition, $y^*(t)$ equals its upper bound $(1-\alpha)w_o$ if $\frac{\partial f}{\partial y}|_{y(t)=(1-\alpha)w_o} < \psi(t)$, Hence, Eq. (28) is obtained. Consequently, candidate dynamical weight $w^*(t) = w_o - y^*(t)$ is obtained as well. □

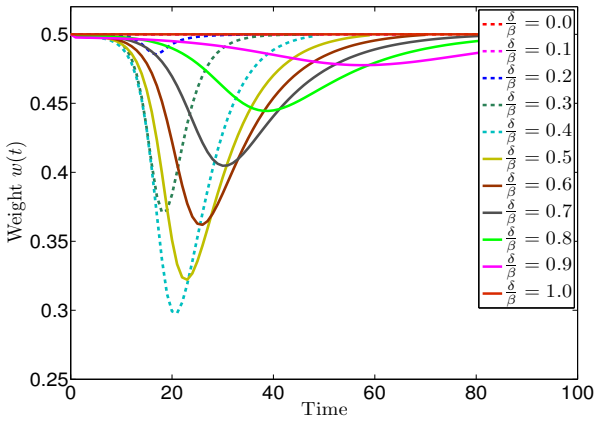

(a) Dynamical weight $w^*(t)$

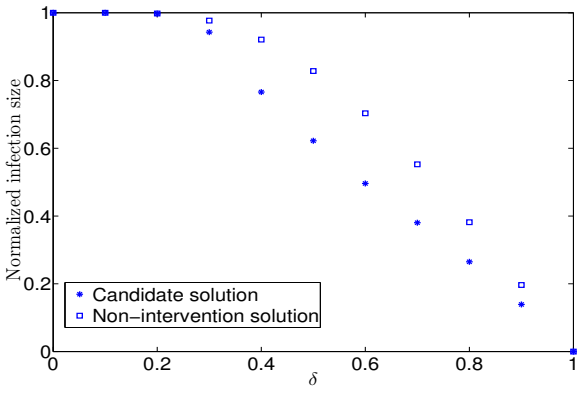

(b) Normalized infection size

FIGURE 1. Numerical evaluation of candidate dynamical weight and candidate normalized infection size for a regular network given different values of cure rate $0 \leq \delta \leq 1$ and constant infection rate $\beta = 1$. The non-intervention policy represents the solution for a constant control function $w(t) = w_o$ as shown in [10].

Figure (1(a)) shows the evaluation of the dynamical weights in time for a homogeneous network in which every node is in contact with two other nodes forming a regular weighted graph. The simulation settings are as follows: 1) initial weight w_o equals 0.5, 2) infection rate β equals 1, 3) the weight reduction cost function is convex with the form $f(z) = z^2$, and 4) $\alpha = 0.1$, $S(0) = 0.8$ and $I(0) = 0.2$. We select the value of β to be $\frac{1}{\lambda_1}$ where λ_1 is the maximum eigenvalue of the undirected weighted network (in our case $\lambda_1 = d_{reg} w_o = 1$ where $d_{reg} = 2$ is the degree of the regular weighted graph). Every curve in the figure represents the evaluation of

the optimal control problem for a given cure rate δ value ($0 \leq \delta \leq 1$). Thus, the Figure shows that the amount of weight reduction increases ($w_o - w(t)$ increases) for $0 \leq \delta \leq 0.4$, and then the weight reduction decreases ($w_o - w(t)$ decreases) for $0.5 \leq \delta \leq 1$. In addition, Figure (1(b)) shows the numerical evaluations for the total fraction of infection cases given different cure rate values $0 \leq \delta \leq 1$ and a constant infection rate $\beta = 1$ for both the non-intervention policy and candidate solution. The non-intervention policy represents the solution when the contact weight is constant $w(t) = w_o$, and the normalized infection size is given by the solution of the equation $1 - s(0)e^{\frac{-(1-s_\infty)\beta}{\delta}}$ as reported by Daley and Gani in [10] where s_∞ and $s(0)$ represent the final and initial fraction of susceptible population in homogeneous networks, respectively. Ultimately, the candidate solution has a lower fraction of infection than the non-intervention policy. We also notice that for small and large values of cure rate, the candidate solutions coincide with the corresponding non-intervention solutions. To clarify, two factors tend to reduce the total infection size, the cure rate and the weight reduction. Meanwhile, there is a tradeoff between their roles in reducing the infection size. In fact, a large cure rate leads to reduced number of infections, and hence the weight reduction becomes less effective; however, a very small cure rate leads to a large number of infections, because the infection process is stronger than the cure process. Hence, the weight reduction becomes less effective. For intermediate values of cure rates, we find that the weight reduction is very effective. Overall, both the weight reduction and the cure process together minimize the total infection size. The same effect is observed for large value of infection rate, which decreases the effective cure rate, and for small values of infection rate, which increases the effective cure rate. For example, for a given cure rate in Figure (1(a)), the dynamical behavior of the weight is described as follows: During the early phase of the epidemic spreading in the population, few nodes are infected, and hence the weight reduction is not effective; however, when the infection size increases, the weight reduction becomes more effective. When the infection process becomes less dominant, the weight reduction decreases due to the exponential decay of infection size, which is a property of the SIR model. Such behavior of the dynamical weight is expected due to the concavity of $\psi(t)$ in Eq. (28).

5. **Computational heuristics.** The candidate solution, obtained through the centralized optimal control framework, requires the global knowledge of the probability of infection for each node and the amount of contact reduction of each link. From implementation point of view, the candidate solution requires large efforts. Therefore, we introduce two heuristics, which require local knowledge of infection to reduce the contact weights with the infectious neighbors. Each heuristic has a distinct control function reflecting a behavioral response to the spread of epidemics. Before we delve into the structure of each heuristic, we define the infection level between every pair of nodes who are in contact, $I_{nm}(t)$, as the probability that node m becomes infected because of being in contact with an infected neighbor n

$$\frac{dI_{nm}(t)}{dt} = \beta S_m(t) w_{m,n}(t) I_n(t) - \delta I_{nm}(t). \tag{30}$$

Also, we define the infection threshold $\bar{I}$ as an infection level that if the infection level between infected neighbor node n and node m, $I_{nm}(t)$, is greater than $\bar{I}$ ($I_{nm}(t) > \bar{I}$), the control function is triggered resulting in reduction of contact weight $w_{m,n}(t) \leq w_o$. Based on the definition of the infection level $I_{nm}(t)$ and

TABLE 2. Proposed Bang-Bang controller heuristic

Weight equation	Condition
$w_{m,n}(t) = w_{m,n}(0)$	**if** $\bar{I} \geq I_{nm}(t)$, $t \leq T_b$
$w_{m,n}(t) = \alpha w_o$	**if** $\bar{I} < I_{nm}(t)$, $T_b \leq t \leq T_e$
$w_{m,n}(t) = w_o$	**if** $\bar{I} \geq I_{nm}(t)$, $t \geq T_e$

the infection threshold $\bar{I}$, we define the structure of each heuristic in the following subsections:

5.1. **Bang-Bang controller heuristic.** In this heuristic, once the infection probability of node m due to infection from neighbor n, $I_{nm}(t)$, exceeds the predefined infection threshold $\bar{I}$, the initial weight $w_{m,n}(0)$ reduces to the minimum social level $\alpha w_{m,n}(0)$ during the time period $[T_b,\ T_e]$ in which $I_{nm}(t) > \bar{I}$. As long as $I_{nm}(t) \leq \bar{I}$, the contact weight from node m to node n $w_{m,n}(t)$ does not change from its normal value $w_{m,n}(0)$. Figure 2(a) and Table 2 shows mechanism of the Bang-Bang controller heuristic. The Bang-Bang controller reflects the node's immediate response that once a node receives the infection from one or more infected neighbors, the node reduces its contact weight with the infected neighbors to the minimum social level. This heuristic also represents a type of homogeneous mitigation strategy in which the mitigation function (weight reduction profile) is the same among all the nodes; however, every pair of nodes decides the start time and the duration during which the contact weight is sharply reduced to its minimum level.

5.2. **Piecewise nonlinear controller heuristic.** The proposed control function is inspired by the candidate dynamical contact weight for homogeneous networks that is obtained using the optimal control theory. As shown in Section 4.2, during the early phase of epidemic, the candidate contact weight is the normal weight w_o, and later when number of infected cases increases, contact weight is reduced nonlinearly. When number of infected decreases, normal contact weight w_o is retrieved nonlinearly. Therefore, we attempt to emulate the candidate weight reduction behavior such that each node reduces its contact weight with the infect neighbor in a decentralized way. In addition, unlike to hte sharp contact weight transition in Bang-Bang control function, piecewise nonlinear control function represents a continuous weight transition. Consequently, the proposed contact weight is a nonlinearly decreasing function in time followed by a nonlinearly increasing function. The nonlinear decreasing contact weight function depends on the infection rate β. The normal contact weight w_o between node m and infected neighbor n is continuously reduced during the time period $[T_b,\ T_e]$ in which the infection level $I_{nm}(t)$ is greater than the infection threshold $\bar{I}$. When the infection level $I_{nm}(t)$ becomes smaller than the infection threshold $\bar{I}$, the normal contact weight w_o is retrieved continuously through a nonlinear increasing function. The node decreases and retrieves the contact weight with its infected neighbor(s) according to the rate of change controller differential equations $\frac{dw_{m,n}(t)}{dt}$ presented in table 3.

The motivation to propose this specific nonlinear weight controller is as follows:

- During the early phase of the spread of an epidemic, the infection size is very small, and therefore, nodes do not change their contact levels $\frac{dw_{m,n}(t)}{dt} = 0 \Rightarrow w_{m,n}(t) = w_{m,n}(0)$.

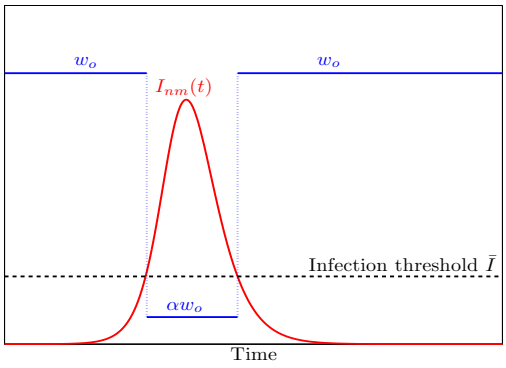

(a) Bang-Bang heuristic

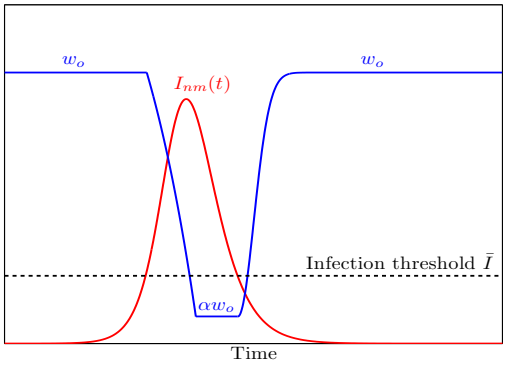

(b) Piecewise nonlinear heuristic

FIGURE 2. Demonstration of the heuristics mechanism. In Bang-Bang heuristic, when the infection between two neighbor nodes $I_{nm}(t)$ increases above the infection threshold $\bar{I}$ ($t = T_b$), the contact weight is reduced from its normal value w_o to the minimum value αw_o. When the infection decreases below the infection threshold at time $t = T_e$, the normal weight is retrieved $w(t) = w_o$. In piecewise nonlinear heuristic, the contact reduction follows a nonlinear function in the time interval $[T_b,\ T_e]$ as shown in table 3 . If the reduced contact weight reaches the minimum level αw_o at time $t < T_e$, the reduce contact weight becomes constant $w(t) = w_o$ as shown in Figure 2(b). When the infection decreases below the infection threshold at time $t = T_e$, the normal weight is retrieved nonlinearly as shown in table 3.

TABLE 3. Proposed piecewise nonlinear controller heuristic

weight rate equation	Condition
$\frac{dw_{m,n}(t)}{dt} = 0, w_{m,n}(t) = w_{m,n}(0)$	**if** $\bar{I} \geq I_{nm}(t), t \leq T_b$
$\frac{dw_{m,n}(t)}{dt} = -\beta^2(w_{m,n}(0)(1-\alpha))(e^{\beta(t-T_b)})$	**if** $\bar{I} < I_{nm}(t),\ T_b \leq t \leq T_e$
$\frac{dw_{m,n}(t)}{dt} = 0$	**if** $\bar{I} < I_{nm}(t),\ T_b < t \leq T_e$, $w_{m,n}(t) = \alpha w_{m,n}(0)$
$\frac{dw_{m,n}(t)}{dt} = (w_{m,n}(0) - w_{m,n}(t))(1 - e^{-\delta(t-T_e)})$	**if** $\bar{I} \geq I_{nm}(t), t \geq T_e$

- Due to a large susceptible population, the spread of the epidemic strengthens, and the infection size starts to increase. Consequently, every node m decreases contact level with each neighbor n according to the infection level $I_{nm}(t)$.
- If a neighbor n is persistently highly infected($\bar{I} < I_{nm}(t)$) and meanwhile the contact weight $w_{m,n}(t)$ reaches its minimum level $\alpha w_{m,n}(0)$, the contact weight remains constant ($\frac{dw_{m,n}(t)}{dt} = 0 \Rightarrow w_{m,n}(t) = \alpha w_{m,n}(0)$) until the infection level $I_{nm}(t)$ becomes lower than the infection threshold.
- When the mitigation time ends ($t > T_e$), nodes recover their contacts following a nonlinear increasing function, which is proportional to the cure rate δ until their initial contact levels are retrieved ($w_{m,n}(0)$).

Why these heuristics are proposed? We know that the candidate solution requires global knowledge of the infection probabilities of the nodes and the amount of weight reduction of the links, while each heuristic requires the local knowledge of the infection probability of the neighbor(s). Bang-Bang heuristic represents a trivial behavioral response that each node reduces its contact with the infected neighbor(s) to the lowest contact level. The simplicity of Bang-Bang heuristic comes at the expense of large weight reduction cost as we show in Section 6 that Bang-Bang heuristic incures highest weight reduction cost. Piecewise nonlinear heuristic has a more intelligent weight reduction strategy, which aims to reduce both the infection cost and the weight reduction cost; However, due to continuously reducing the contact weights, the efforts required to implement the piecewise nonlinear heuristic is larger than the efforts required to implement Bang-Bang heuristic. Therefore, the two heuristics have a tradeoff between the overall cost and the implementation efforts.

6. Numerical evaluation.

We performed extensive simulations on three types of networks to evaluate the proposed heuristics. The first type is a small 5-node network to evaluate the performance of the heuristics with respect to the candidate solution. The small network size is suitable to obtain the candidate solution in reasonable running time. On the other hand, it is hard to obtain the candidate solution for large networks in polynomial running time. The second type is preferential attachment networks, [3], and the third type is a survey-based contact network [38]. In addition, we briefly discuss the differences between our approaches and static social distancing mitigation methods.

6.1. Candidate and heuristic solutions.

To justify the performance of the heuristics with respect to the candidate solution, the optimization problem and the heuristics were applied to a small network with five nodes with initial contact rate $w_{m,n}(0)$ equals 0.5 as shown in Figure 3. The candidate solution and the heuristic solutions were found given different cure rates ($0.1 \leq \delta \leq 0.9$). In Figure 4, we

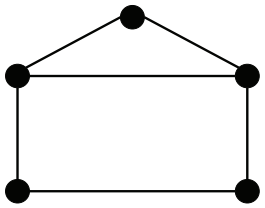

FIGURE 3. A 5-node network

report the total cost, the weight reduction cost and the normalized infection size. The total cost for the candidate solution represents a lower bound while Bang-Bang heuristic has the maximum total cost. For a large range of cure rate, the total cost provided by the heuristics are close to the candidate solutions except for a small cure rate ($\delta = 0.1$), where the total cost of the heuristic solutions diverge from the candidate solution. The infection size for the piecewise nonlinear heuristic is lower than the infection size provided by the optimization problem and Bang-Bang heuristic. However, the weight reduction has the lowest cost in the candidate solution compared to the weight reduction cost from the two heuristics. Therefore, we conclude that the optimal control approach balances the infection cost and the weight reduction cost. In Figure 4, we also report the best infection threshold $\bar{I}^{best}$ at which the infection reduction has the lowest value for both the Bang-Bang and piecewise nonlinear heuristics given different cure rates. We notice that the best infection threshold is inversely proportional to the cure rate, and we make the same observation for large networks as shown in Section 6.2.

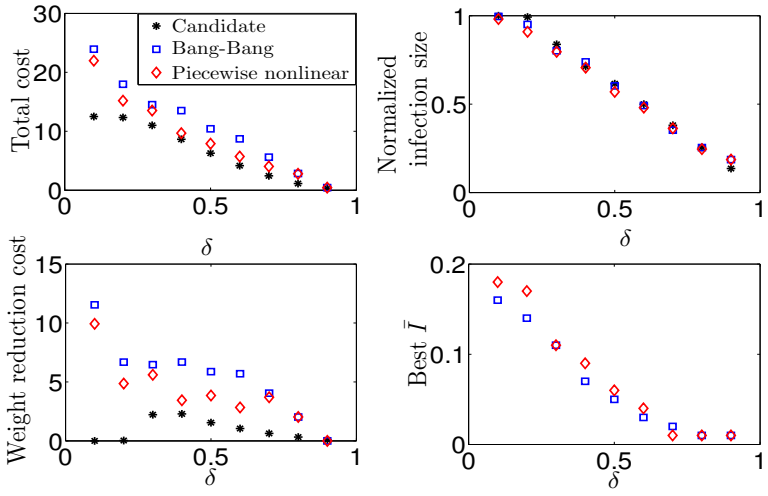

FIGURE 4. The numerical evaluation of the candidate and heuristic solutions for a 5-node network given different cure rate δ.

6.2. **Preferential attachment networks.** Next, the proposed heuristics were applied to preferential attachment networks. Different cure rates δ, and infection

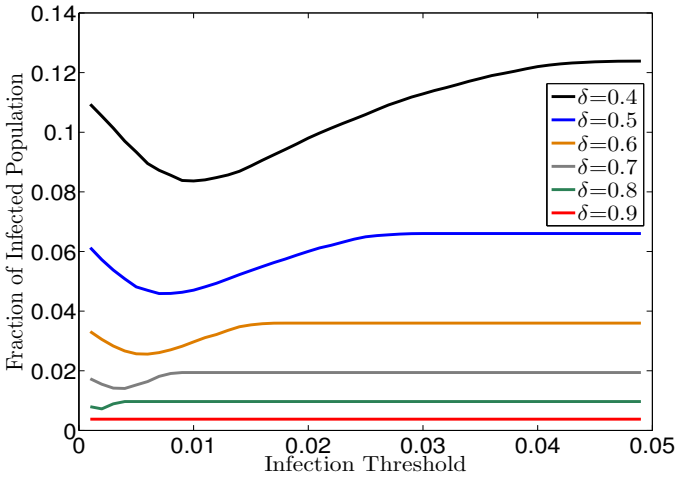

(a) Bang-Bang controller

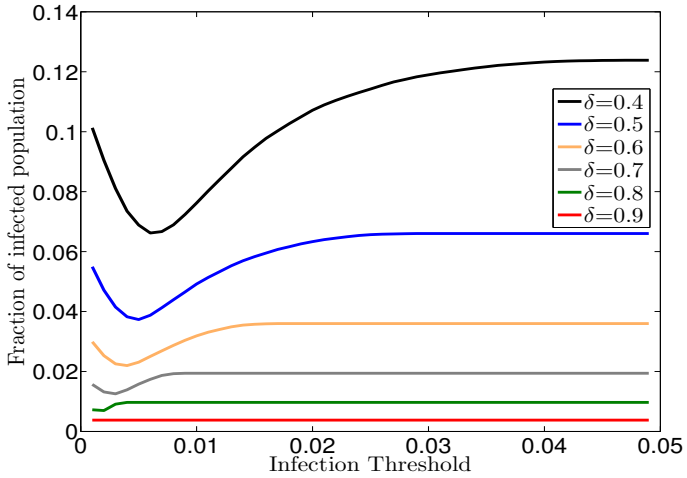

(b) Piecewise nonlinear controller

FIGURE 5. Numerical evaluation of the normalized infection size for both the Bang-Bang controller heuristic and the piecewise nonlinear controller heuristic given preferential attachment networks, different cure rate $0.4 \leq \delta \leq 0.9$ and different infection threshold $\bar{I}$. The numerical evaluation is averaged over 20 runs. The best $\bar{I}$ is the value at which the normalized infection size is minimal.

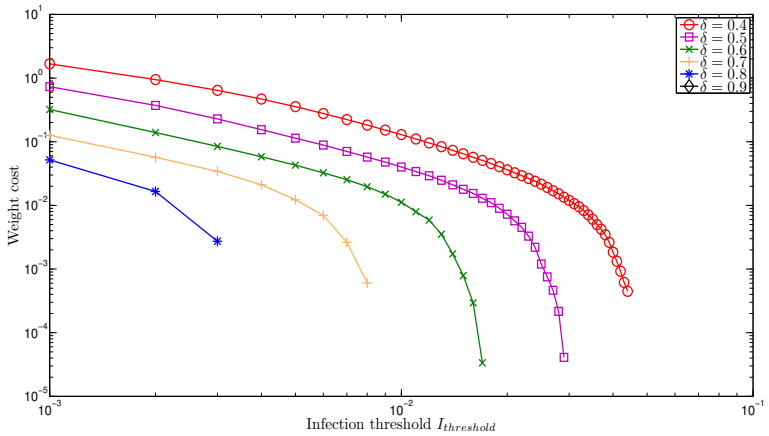

(a) Bang-Bang controller

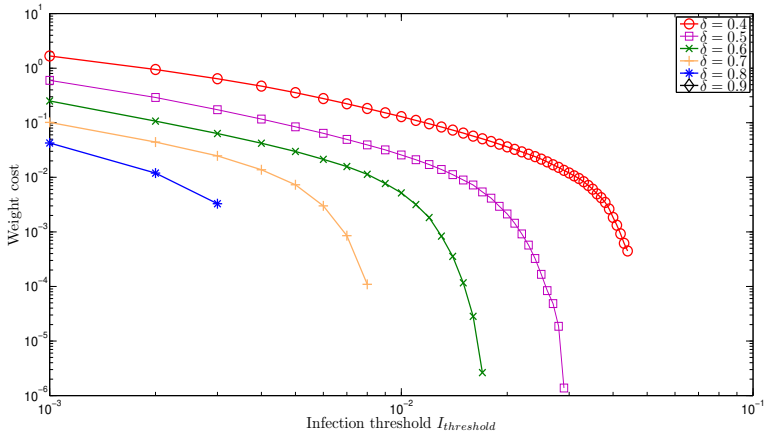

(b) Piecewise nonlinear controller

FIGURE 6. Numerical evaluation of the weight reduction cost for both the Bang-Bang controller heuristic and the piecewise nonlinear controller heuristic given preferential attachment networks, different cure rate $0.4 \leq \delta \leq 0.9$ and different infection threshold $\bar{I}(I_{threshold})$. The numerical evaluation is averaged over 20 runs.

threshold $\bar{I}$ were used with every heuristic, while the infection rate β was set to be equal to the reciprocal of the epidemic threshold $\frac{1}{\lambda_1}$ [42], where λ_1 is the maximum eigenvalue of the original weighted contact network. Figures 5(a) and 5(b) show the normalized infection size for different infection thresholds $\bar{I}$ and cure rates $0.4 \leq \delta \leq 0.9$ for Bang-Bang and piecewise nonlinear controller heuristics,

respectively. All results were averaged over 20 different preferential attachment networks, and each network has 10^4 nodes with initial contact weight value equals $w_{m,n}(0) = 0.5$ and minimum contact weight equals $\alpha w_{m,n}(0) = 0.05$. For Bang-Bang control function, as shown in Figure 5(a), for a given δ and small $\bar{I}$, the infection size decreases until it reaches a minimum value, and it increases for higher values of $\bar{I}$ until it reaches its highest value at which the mitigation strategy is no longer effective. Therefore, small values as well as high values of $\bar{I}$ are not effective to reduce infection cases. In addition, as shown in Figure 6(a), small values as well as high values of $\bar{I}$ incur extreme high and low weight reduction costs, respectively. Hence, for a given δ, there is a best $\bar{I}^{best}$ value at which the infection size has the lowest value as shown in Figure 5(a) with a moderate weight reduction cost as shown in Figure 6(a). The above observations correlate with the finding by Bondes *et al.* [7] that the optimal immunization investment is maximized for intermediate values of infection probabilities, while the immunization investment is less effective for low and high infection probabilities values. For instance, for $\delta = 0.9$, the weight reduction cost is 0 (not shown on the log scale) for any $\bar{I} \geq 10^{-3}$ values. The same observations were obtained for the piecewise nonlinear controller heuristic as shown in Figures 5(b) and 6(b).

Below, we summarize the numerical evaluation obtained from testing both heuristics as follows:

- As the cure rate δ increases, the best infection threshold $\bar{I}^{best}$ decreases. To clarify, high cure rate represents short infection time, and hence the probability that a susceptible node receives the infection from an infected neighbor decreases. Therefore, smaller values of $\bar{I}$ for the mitigation strategy to be effective are required.
- The normalized infection size for the piecewise nonlinear controller heuristic is smaller than the normalized infection size for Bang-Bang controller heuristic at every cure rate. Furthermore, the incurred weight reduction cost from the piecewise nonlinear controller heuristic is lower than the incurred cost from the Bang-Bang controller heuristic as shown in Figures 6(a) and 6(b). Therefore, the piecewise nonlinear controller heuristic outperforms the well-known Bang-Bang controller in both the infection size and weight cost. However, every heuristic has different applications. For example, in Bang-Bang control function, nodes simply change their activities to the minimum level with nodes who are suspected to have the infection. In the piecewise nonlinear control function, nodes prefer to maintain their contacts to levels that not only allow them to interact with other nodes in the community, but that also keep them to be cautious about receiving the infection from their infected neighbors.

6.3. **Survey-based weighted contact network.** We applied both Bang-Bang and piecewise nonlinear heuristics to a survey-based contact network to study the effect of the mitigation strategies on total infection size. The contact network was created through a survey to study the spread of epidemics in rural regions [38]. The survey was conducted in Clay Center, the county seat of Clay County in the State of Kansas, and the network was created based on the responses of Clay Center residents. The survey included questions about the number of times that the respondents visit three main places, {R,W,G}, and questions about three levels of contact that each respondent i makes per day. The three levels of contact were defined as follows. 1) *Proximity contact* $w_{PX,i,j}$, which happens when another

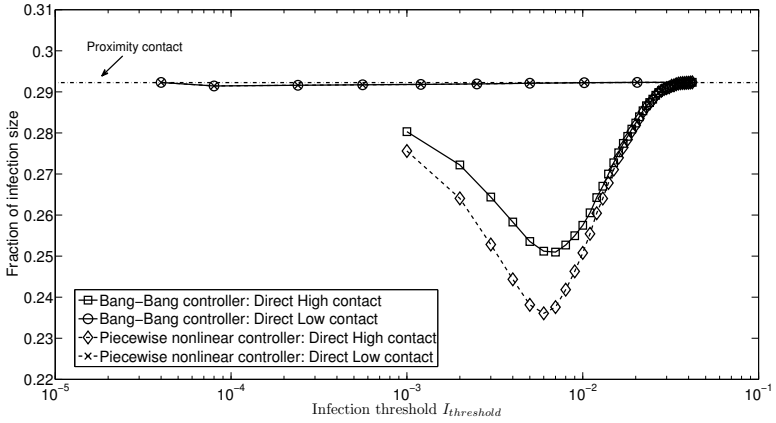

FIGURE 7. Numerical evaluation of the Bang-Bang and the piecewise nonlinear heuristics for the three types of contacts in the survey-based contact network given the infection rate $\beta = 0.36$, and the cure rate $\delta = 0.4$.

person is passing within five feet, 2) *Direct Low contact* $w_{DL,i,j}$, which happens when a person is directly touching another person for a short time period, and 3) *Direct High contact* $w_{DH,i,j}$, which happens when a person is directly touching another person for a long time period. We used the survey responses to create a weighted contact network with 138 nodes (respondents) and 9222 links (contacts). Based on the responses of the residents, we formulated the link weights, which are functions of the common locations that the nodes visit, and the frequency of daily contacts and proximity. The weight between node i and node j is the average of the three contact levels. For contact type x, we proposed the following equation:

$$w_{x,i,j} = (1 - (1 - \mu_{i,j}\pi_x)^{n_{x,i}})(1 - (1 - \mu_{i,j}\pi_x)^{n_{x,j}}) \tag{31}$$

where π_x is a constant that depends on the level of contact x, $n_{x,i}$ is the frequency of contact level x of respondent i, and $\mu_{i,j}$ quantifies the location responses for both respondents i and j as follows:

$$\mu_{i,j} = \frac{1 + l_{i,j}}{1 + d} \tag{32}$$

where d is the total number of locations, and $l_{i,j}$ represents the number of common locations that respondents i and j used to visit. The total contact rate between nodes i and j is as follows:

$$\frac{w_{PX,i,j} + w_{DL,i,j} + w_{DH,i,j}}{3}.$$

For more details about the survey questions and the link weights, we refer the reader to the work in [38].

Bang-Bang and piecewise nonlinear heuristics were applied to every type of contact between nodes i and j. For every heuristic applied to a certain type of contact, say $w_{x,i,j}$, the minimum contact level is $\alpha w_{x,i,j}$. For example, when Bang-Bang

heuristic was applied to proximity contact, only the proximity contact rate was reduced. Similarly, the mitigation strategy was applied to the direct-low and direct-high contacts. The same mitigation strategy process was used with the piecewise nonlinear controller. For different values of infection thresholds, Figure 7 shows that the mitigation of every type of contact has a different impact on the total size of infection. To clarify, when the mitigation strategy is applied to direct high contacts, the largest impact on the total infection size is obtained; however, the mitigation strategy has no impact on the proximity contact. In addition, the piecewise nonlinear heuristic is more effective on the direct high contact than the Bang-Bang heuristic.

6.4. **Static social distancing.** We discuss the differences between the proposed heuristic approaches and static social distancing mitigation strategy. Consider that the normal contact weights among nodes have the same value, say w_o. In static social distancing, the contact weight is reduced to its lowest level αw_0 all the time. In this case, the epidemic threshold increases from $\frac{1}{w_o\lambda_1}$ to $\frac{1}{\alpha w_o\lambda_1}$, which in turn reduces the number of infection cases for any effective infection rate $\frac{\beta}{\delta}$ greater than the epidemic threshold. Therefore, static social distancing mitigation strategy reduces the number of infection cases; however, it incurs the maximum weight reduction cost. On the other hand, in the proposed approaches, the contact weight dynamically changes between its maximum and minimum values w_o and αw_o, respectively. Hence, the contact network does not incur the maximum weight reduction cost value, yet the number of infection cases is reduced. Therefore, our approaches outperform the static social distancing mitigation strategy in balancing minimization of the number of infection cases and minimization of weight reduction cost.

7. **Discussion.** This study aims to integrate the optimal control theory with the SIR compartmental model to minimize the total infection and the weight reduction cost in a contact network during the spread of an epidemic. Differently from the quarrantine scenario, we assume that the weight reduction is bounded from below by a minimum contact level αw_o that is greater than 0. The optimal control theory provides a candidate solution for the state of each node and the amount of weight reduction cost for every contact. It shows that every contact is reduced nonlinearly when the infection risk is high, and then the original contact weight is retrieved nonlinearly when the infection risk becomes low. This solution proves that even if the contact weights are not set to 0 during the wave of an epidemic (as in the quarrantine scenario), the infection is minimized and the contact weights are reduced intelligently to minimize the weight reduction cost. The candidate solution is obtained through a centralized method, which requires the global knowledge of the infection state of each individual in the contact network such that a contact reduction decision is made based on minimization the overall cost. The contact reduction between a pair of nodes takes place based on not only the infection state of that pair of nodes but also on the infection state of all nodes and the amount of overall contact reduction in the network. Therefore, the effort to implement the candidate solution is high. On the other hand, the proposed heuristics aim to avoid the requirement of global knowledge of the infection state of all nodes in the contact network. Each heuristic provides a solution in a decentralized way that only requires local knowledge of the infection state of the node's neighbors. The two heuristics present two different dynamical responses to the spread of epidemics. In Bang-Bang heuristic, each node reduces its contact(s) with the infectious neighbor(s) to

the minimum αw_o if the infection level increases above the predefined threshold $\bar{I}$. The amount of effort that is required by every individual is less than the amount of efforts to obtain a candidate solution using the optimal control theory. This heuristic reflects the human response during the wave of an epidemic. The piecewise nonlinear heuristic represents another human response which requires high efforts to continuously observing the infection state of the neighbor(s) and to continuously reducing the contact weights. Therefore, the candidate solution requires the highest efforts in observing the infection states of all the nodes, followed by the piecewise nonlinear heuristic solution which requires observing the infection state of the local neighbor(s) and gradient contact reduction with the local neighbor(s), and finally the Bang-Bang heuristic solution requires the least efforts because a nodes has to observe the infection state of the local neighbor(s) and reducing the contact weights to a constant value during the period of time of high infection risk.

The optimal control theory and the heuristics influence the outcomes of the epidemic for moderate values of infection rates and cure rates. For extreme values of infection rates and cure rates, the optimal control theory and the heuristics have no effect on reducing the total infected cases in the contact network.

8. **Summary.** Below, we summarize our findings as follows:

- *In homogeneous networks, the candidate contact weights are adaptive:* To balance minimization of the weight reduction cost and number of infection cases, weights decrease nonlinearly from their normal values when the epidemic spreading process overwhelms the network, and then the normal contact weight values are retrieved when the curing process overcomes the infection process
- *The optimal control problem addresses the relationship between the effective cure rate and the optimal control function:* For intermediate values of effective cure rate, the values of weights are reduced dramatically from their normal values.
- *The piecewise nonlinear controller outperforms the Bang-Bang controller:* The number of infected cases and the incurred weight reduction cost obtained by the nonlinear heuristic are lower than those obtained by the Bang-Bang controller.
- *The most effective strategy is the mitigation of direct-high contact:* With a nonlinear controller, the mitigation strategy of the direct-high contact is the most effective strategy compared to the proximity and direct-low contacts.

9. **Conclusions and future work.** In this paper, we presented the adaptive contact weighted networks, which minimize a linear combination of the total number of infection cases and the weight reduction cost when an epidemic spreads in a social contact network. We briefly presented the network-based SIR approach for weighted networks, and we applied the optimal control theory to find the candidate adaptive network. In addition, we analytically found the candidate adaptive homogeneous weighted networks, and we discussed the role of effective cure rate and weight reduction to minimize both the amount of weight reduction and the total number of infection cases. Moreover, we proposed two different heuristics to find near-optimal solutions in a decentralized way. The two heuristics are based on Bang-Bang control function, and piecewise nonlinear control function, respectively. To evaluate the heuristics, we performed extensive numerical simulations

on weighted preferential attachment networks and a survey-based contact network. The results suggested that the piecewise nonlinear controller heuristic is more effective than the well-known Bang-Bang controller in minimizing both the infection cases and the weight reduction cost.

Future work will focus on applying the optimal control theory to contact networks in which the overall contact strength of every node will be adapted to minimize the total infection size. In addition, we will study the effect of the global minimum social level coefficient on the spread of epidemics in contact networks. In addition, we will provide an optimal control approach that addresses the tradeoff between the reward of strengthening the contact within households when a quarrantine scenario is taking place in the contact network, and the cost that may be inquired due to the awareness of every individual within the household. Also, we will apply different numerical optimization methods to minimize a linear combination of the final infection sizes and the weight reductions for every pair of nodes and the total contact weight for every node.

Acknowledgments. This work is partially supported by the National Agricultural Biosecurity Center at Kansas State University, and the National Science Foundation under award number EPS-0919443 and by National Institutes of Health and National Institute of General Medical Sciences - Models of Infectious Disease Agent Study Grant 2U01GM070694-09.

REFERENCES

[1] M. Ajelli et al., *Comparing large-scale computational approaches to epidemic modeling: agent-based versus structured metapopulation models*, BMC Infectious Diseases, **10** (2010), 190.

[2] P. Bajardi et al., *Modeling vaccination campaigns and the Fall/Winter 2009 activity of the new A(H1N1) influenza in the Northern Hemisphere*, Emerging Health Threats Journal, **2** (2009), e11.

[3] A.-L. Barabási and R. Albert, *Emergence of scaling in random networks*, Science, **286** (1999), 509–512.

[4] C. Barrett, K. Bisset, S. Eubank, X. Feng and M. Marathe, *EpiSimdemics: An efficient and scalable framework for simulating the spread of infectious disease on large social networks*, in "Proceedings of SuperComputing 08 International Conference for High Performance Computing," Networking Storage and Analysis. Austin, Texas, November 15-21, (2008).

[5] C. Barrett, K. Bisset, J. Leidig, A. Marathe and M. Marathe, *An integrated modeling environment to study the co-evolution of networks, individual behavior, and epidemics*, AI Magazine, **31** (2009), 75–87.

[6] H. Behncke, *Optimal control of deterministic epidemics*, Optimal Control Applications and Methods, **21** (2000), 269–285.

[7] M. Bondes, D. Keenan, A. Leidner and P. Rohani, *Higher disease prevalence can induce greater sociality: A game theoretic coevolutionary model*, The Society for the Study of Evolution: International Journal of Organic Evolution, **59** (2005).

[8] V. L. Brown and K. A. J. White, *The role of optimal control in assessing the most cost-effective implementation of a vaccination programme: HPV as a case study*, Mathematical Biosciences, **231** (2011), 126–134.

[9] V. Colizza, A. Barrat, M. Barthelemy and A. Vespignani, *Epidemic predictability in meta-population models with heterogeneous couplings: The impact of disease parameter values*, Int. J. Bifurcation and Chaos, **17** (2007), 2491–2500.

[10] D. J. Daley and J. Gani, "Epidemic Modelling: An Introduction," Cambridge, Studies in Mathematical Biology, 1999.

[11] F. Darabi, F. N. Chowdhury and C. M. Scoglio, *On the existence of a threshold for preventive behavioral responses to suppress epidemic spreading*, Scientific Reports 2, Article number 632, 2012

[12] W. Dong, K. Heller and A. Pentland, *Modeling infection with multi-agent dynamics*, in "Social Computing, Behavioral-Cultural Modeling And Prediction," (Ed. S. Yang), Berlin Heidelberg, Springer, **7227** (2012), 172–179.
[13] S. Eubank et al., *Modelling disease outbreaks in realistic urban social networks*, Nature, **429** (2004), 180–184.
[14] E. P. Fenichel et al., *Adaptive human behavior in epidemiological models*, Proceedings of the National Academy of Sciences, **108** (2011), 6306–6311.
[15] G. A. Forster and C. A. Gilligan, *Optimizing the control of disease infestations at the landscape scale*, Proceedings of the National Academy of Sciences, **104** (2007), 4984–4989.
[16] D. Gao and S. Ruan, *An SIS patch model with variable transmission coefficients*, Mathematical Biosciences, **232** (2011), 110–115.
[17] T. Germann, K. Kadau, I. Longini and C. Macken, *Mitigation strategies for pandemic influenza in the United States*, Proceedings of the National Academy of Sciences, **103** (2006), 5935–5940.
[18] T. Gross and B. Blasius, *Adaptive coevolutionary networks: A review*, Journal of the Royal Society Interface, **5** (2010), e11569.
[19] T. Gross, C. J. D. D'Lima and B. Blasius, *Epidemic dynamics on an adaptive network*, Phys. Rev. Lett., **96** (2006), 208701.
[20] M. Hashemian, W. Qian, K. G. Stanley and N. D. Osgood, *Temporal aggregation impacts on epidemiological simulations employing microcontact data*, BMC Medical Informatics and Decision Making, **12** (2012), 132.
[21] C. Jiang and M. Dong, *Optimal measures for SARS epidemics outbreaks*, IEEE Intelligent Control and Automation WCICA, (2006).
[22] M. H. R. Khouzani, S. Sarkar and E. Altman, *Optimal control of epidemic evolution*, Proceedings of IEEE INFOCOM 2011, Shanghai, China, (2011).
[23] I. Kiss, D. Green and R. Kao, *The effect of network mixing patterns on epidemic dynamics and the efficacy of disease contact tracing*, Journal of the Royal Society Interface, **5** (2008), 791–799.
[24] C. Lagorio et al., *Quarantine generated phase transition in epidemic spreading*, Phys. Rev. E, **83** (2011), 026102,.
[25] A. Marathe, B. Lewis, J. Chen and S. Eubank, *Sensitivity of household transmission to household contact structure and size*, PLoS ONE, **6** (2011), e22461.
[26] V. Marceau et al., *Adaptive networks: Coevolution of disease and topology*, Phys. Rev. E, **82** (2010), 036116,
[27] M. L. N. Mbah and C. A. Gilligan, *Resource allocation for epidemic control in metapopulations*, PLoS ONE, **6** (2011), e24577.
[28] M. L. N. Mbah and C. A. Gilligan, *Optimization of control strategies for epidemics in heterogeneous populations with symmetric and asymmetric transmission*, Journal of Theoretical Biology, **262** (2010), 757–763.
[29] P. V. Mieghem, J. S. Omic and R. E. Kooij, *Virus spread in networks*, IEEE/ACM Transaction on Networking, **17** (2009), 1–14.
[30] Y. Moreno, R. Pastor-Satorras and A. Vespignani, *Epidemic outbreaks in complex heterogeneous networks*, Eur. Phys. J. B, **26** (2002), 521–529.
[31] M. E. J. Newman, *The structure and function of complex networks*, SIAM Review, **45** (2003), 167–256.
[32] L. S. Pontryagin et al., *The mathematical theory of optimal processes*, Interscience, **4** (1962).
[33] B. Prakash, H. Tong, N. Valler, M. Faloutsos and C. Faloutsos, *Virus propagation on time-varying networks: theory and immunization algorithms*, ECML-PKDD 2010, Barcelona, Spain 2010.
[34] O. Prosper, O. Saucedo, D. Thompson, G. Torres-Garcia, X. Wang and C. Castillo-Chavez *Modeling control strategies for concurrent epidemics of seasonal and pandemic H1N1 influenza*, **8** (2011), 141–170.
[35] T. Reluga, *Game theory of social distancing in response to an epidemic*, PLOS Computational Biology, **6** (2010), e1000793.
[36] T. Reluga and A. Galvani, *A general approach to population games with application to vaccination*, Mathematical Biosciences, **230** (2011), 67–78.
[37] R. E. Rowthorn, R. Laxminarayan and C. A. Gilligan, *Optimal control of epidemics in metapopulations*, Interface Journal of the Royal Society, **6** (2009), 1135–1144.

[38] C. Scoglio et al., *Efficient mitigation strategies for epidemics in rural regions*, PLoS ONE, **5** (2010), e11569.

[39] J. Stehle, N. Voirin, A. Barrat, C. Cattuto, V. Colizza, L. Isella, C. Regis, J-F. Pinton, N. Khanafer, W. Van den Broeck and P. Vanhems, *Simulation of an SEIR infectious disease model on the dynamic contact network of conference attendees*, BMC Med, **9** (2011).

[40] S. Towers and Z. Feng, *Pandemic H1N1 influenza: Predicting the course of a pandemic and assessing the efficacy of the planned vaccination programme in the United States*, Euro Surveillance, **14** (2009) .

[41] E. Volz and L. A. Meyers, *Susceptible-infected-recovered epidemics in dynamic contact networks*, Proceedings of the Royal Society B, **274** (2011), 2925–2934.

[42] M. Youssef and C. Scoglio, *An individual-based approach to SIR epidemics in contact networks*, JTB: Journal of Theoretical Biology, Elsevier, **283** (2011), 136–144.

Received September 17, 2012; Accepted March 16, 2013.

E-mail address: myoussef@vbi.vt.edu
E-mail address: caterina@ksu.edu